

## Rhombohedral–Tetragonal Phase Boundary with High Curie Temperature in $(1-x)\text{BiCoO}_3$ – $x\text{BiFeO}_3$ Solid Solution

This content has been downloaded from IOPscience. Please scroll down to see the full text.

2008 Jpn. J. Appl. Phys. 47 7579

(<http://iopscience.iop.org/1347-4065/47/9S/7579>)

View [the table of contents for this issue](#), or go to the [journal homepage](#) for more

Download details:

IP Address: 130.239.20.174

This content was downloaded on 31/08/2014 at 02:19

Please note that [terms and conditions apply](#).

## Rhombohedral–Tetragonal Phase Boundary with High Curie Temperature in $(1 - x)\text{BiCoO}_3$ – $x\text{BiFeO}_3$ Solid Solution

Masaki AZUMA, Seiji NIITAKA\*, Naoaki HAYASHI<sup>1</sup>, Kengo OKA, Mikio TAKANO<sup>†</sup>, Hiroshi FUNAKUBO<sup>2</sup>, and Yuichi SHIMAKAWA

*Institute for Chemical Research, Kyoto University, Uji, Kyoto 611-0011, Japan*

<sup>1</sup>*Graduate School of Human and Environmental Sciences, Kyoto University, Kyoto 606-8501, Japan*

<sup>2</sup>*Department of Innovative and Engineered Materials, Tokyo Institute of Technology, J2-1508, 4259 Nagatsuta-cho, Midori-ku, Yokohama 226-8502, Japan*

(Received June 9, 2008; accepted July 14, 2008; published online September 19, 2008)

The crystal structure change of the solid solution  $\text{BiCo}_{1-x}\text{Fe}_x\text{O}_3$  was investigated in order to determine the phase boundary between tetragonal  $\text{BiCoO}_3$  and rhombohedral  $\text{BiFeO}_3$ . It was found that  $\text{BiCo}_{1-x}\text{Fe}_x\text{O}_3$  with  $x = 0$  to 0.6 had tetragonal  $\text{BiCoO}_3$  structures, while those with  $x = 0.8$  to 1 had rhombohedral  $\text{BiFeO}_3$  structures at room temperature. The monoclinic  $\sqrt{2}a \times \sqrt{2}a \times a$  phase was found for the  $x = 0.7$  sample. The tetragonal-to-cubic phase transition was first observed at around 700–850 °C in Bi-based perovskite for the  $x = 0.8$  sample. [DOI: 10.1143/JJAP.47.7579]

KEYWORDS: MPB, high-pressure synthesis,  $\text{BiCoO}_3$ ,  $\text{BiFeO}_3$

### 1. Introduction

$\text{PbTiO}_3$ -based piezoelectric materials such as  $\text{PbZr}_x\text{Ti}_{1-x}\text{O}_3$  (PZT) are widely used in actuators and ultrasound transducers. The outstanding piezoelectric property of PZT is due to the high transition temperature ( $T_C$ ) and the presence of a morphotropic phase boundary (MPB) in the solid solution between tetragonal  $\text{PbTiO}_3$  and rhombohedral  $\text{PbZrO}_3$ .<sup>1,2</sup> The high  $T_C$  of 385 °C at the MPB composition which enables the application of PZT in high-temperature devices such as injectors of a diesel engine can be attributed to the high  $T_C$  of  $\text{PbTiO}_3$  with a large tetragonal distortion owing to the  $6s^2$  lone pair of  $\text{Pb}^{2+}$  and the covalent Pb–O bond.<sup>3</sup> The presence of  $\text{Ti}^{4+}$  without a  $d$  electron at the B-site is also believed to be essential for the noncentrosymmetric structure. The tetragonal  $\text{PbTiO}_3$ -type structure can be obtained for a perovskite with a tolerance factor ( $t$ ) larger than 1. A good example is  $\text{BaTiO}_3$ .  $\text{SrTiO}_3$  ( $t \sim 1$ ) is a cubic paraelectric. The replacement of  $\text{Sr}^{2+}$  with the larger  $\text{Ba}^{2+}$  leads to a tetragonal ferroelectric,  $\text{BaTiO}_3$ .<sup>4</sup> The absence of nontoxic alkaline-earth ions larger than  $\text{Ba}^{2+}$  precludes the material design of  $\text{Ti}^{4+}$ -based piezoelectrics in this context. There is no A-site cation other than  $\text{Pb}^{2+}$  with  $6s^2$  lone pairs to increase the tetragonality of  $\text{BaTiO}_3$  because the only rare-earth ion larger than  $\text{Ba}^{2+}$  is radioactive  $\text{Ra}^{2+}$ . However, in 2004, Saito *et al.* reported a novel pentavalent B-site-cation-based material,  $(\text{Li}^+, \text{N}^+, \text{K}^+)(\text{Nb}^{5+}, \text{Ta}^{5+})\text{O}_3$ , with a large piezoelectric coefficient compatible with lead-based compounds.<sup>5</sup> However, alkali metals are unsuitable for the Si-based device process, which is essential for micro electro mechanical systems (MEMS) application. The search for practically useful ferroelectric and piezoelectric perovskites has been limited to systems with  $d^0$  ions such as  $\text{Ti}^{4+}$ ,  $\text{Zr}^{4+}$ ,  $\text{Nb}^{5+}$ , and  $\text{Ta}^{5+}$  at B-sites. The large spontaneous polarization found in thin films of the rhombohedral perovskite  $\text{BiFeO}_3$ , however, suggests that investigations of Bi and Pb perovskites with other transition elements

might lead to new high-performance ferroelectric and piezoelectric materials.<sup>6</sup> The solid solution  $(1 - x)\text{PbTiO}_3$ – $x\text{BiFeO}_3$  exhibits a  $T_C$  of 632 °C at an MPB composition of  $x = 0.7$ .<sup>7</sup> The development of a new piezoelectric material with higher  $T_C$  will lead to new applications such as power conversion from the vibration of the exhaust. To our knowledge, this is the highest  $T_C$  at the MPB composition among binary perovskite systems.<sup>8,9</sup> In  $\text{BiFeO}_3$ ,  $\text{Bi}^{3+}$  plays the same role as  $\text{Pb}^{2+}$  because these ions essentially have the same electronic configuration.  $\text{BiFeO}_3$  and  $\text{PbTiO}_3$  are the only Bi and Pb 3d transition-metal perovskites that can be prepared at ambient pressure.

We have investigated other perovskites stabilized by high-pressure synthesis,<sup>10–15</sup> and found that  $\text{PbVO}_3$ <sup>14</sup> and  $\text{BiCoO}_3$ <sup>15</sup> are isostructural with  $\text{PbTiO}_3$  but have tetragonal distortions ( $c/a = 1.229$  for  $\text{PbVO}_3$  and 1.267 for  $\text{BiCoO}_3$ ) much larger than that of  $\text{PbTiO}_3$  ( $c/a = 1.043$ ). Because of the structural similarities, it is speculated that the solid solution between  $\text{BiCoO}_3$  and  $\text{BiFeO}_3$  is a candidate replacement for PZT. The fabrication of a  $(1 - x)\text{BiCoO}_3$ – $x\text{BiFeO}_3$  thin film was attempted by metalorganic chemical vapor deposition (MOCVD) and it was found that  $x = 0.67$  to 1 samples are obtained as epitaxial thin films.<sup>16</sup> However, the phase relations in the entire composition and temperature range necessary for the determination of the MPB line remain unclear. In this paper, we report the phase diagram of the  $(1 - x)\text{BiCoO}_3$ – $x\text{BiFeO}_3$  system based on high-pressure synthesis and high-temperature powder X-ray diffraction (XRD) studies.

### 2. Experimental Methods

$\text{BiCo}_{1-x}\text{Fe}_x\text{O}_3$  samples were prepared from  $\text{Bi}_2\text{O}_3$ ,  $\text{Co}_3\text{O}_4$ , and  $\text{Fe}_2\text{O}_3$ . The stoichiometric mixtures were charged in gold capsules of 3.6 mm diameter and 5 mm height and were compressed to 4 to 6 GPa followed by heat treatment at 1000 °C for 30 min in a cubic anvil type high-pressure apparatus. 10 mg of oxidizing agent  $\text{KClO}_4$  was added to the top and bottom of the capsule in a separate manner. The obtained samples were crushed and washed with distilled water to remove the remaining KCl. Then large particles that caused the inhomogeneous Debye ring and preferred orientation were removed with a sieve. The

\*Present address: RIKEN (The Institute of Physical and Chemical Research), Wako, Saitama 351-0198, Japan.

†Present address: Institute for Integrated Cell-Material Sciences, Kyoto University c/o Research Institute for Production Development, 15 Shimogamo Morimoto-cho, Sakyo-ku, Kyoto 606-0805, Japan.

crystal structures of the samples at a room temperature for the tetragonal ( $x = 0$ – $0.6$ ) and rhombohedral ( $x = 0.9$  and  $1$ ) phases were refined by the Rietveld analysis of the synchrotron X-ray powder diffraction (SXRD) collected with a large Debye-scherrer camera installed at the beamline BL02B2 of SPring-8.<sup>17)</sup> The software Rietan 2000 was used in the refinement.<sup>18)</sup> SXRD patterns were also collected for the  $x = 0.5$  sample at higher temperature. The high-temperature XRD patterns of the  $x = 0.7, 0.8, 0.9$ , and  $1$  samples were collected with Cu K $\alpha$  radiation using Rigaku RINT 2500 diffractometer since the temperature range of SXRD was limited up to  $600^\circ\text{C}$ .

### 3. Results and Discussion

Figure 1 shows the SXRD patterns of  $\text{BiCo}_{1-x}\text{Fe}_x\text{O}_3$  collected at room temperature. The pattern for the  $x = 0$  sample can be indexed assuming a tetragonal cell of  $a = 0.37306\text{ nm}$  and  $c = 0.47262\text{ nm}$ . The patterns for the  $x = 0.2$ – $0.6$  samples could also be indexed with tetragonal unit cells. The 011 peak of the  $x = 0.7$  sample split into 2, suggesting the symmetry lowering of the crystal structure. This pattern was indexed with a monoclinic cell of  $a = 0.5277\text{ nm}$ ,  $b = 0.5272\text{ nm}$ ,  $c = 0.4685\text{ nm}$  and  $\beta = 91.35^\circ$ . It should be noted that this monoclinic  $\sqrt{2}a \times \sqrt{2}a \times a$  cell is found in the PZT system as a low-temperature phase at the MPB composition.<sup>19)</sup> The patterns of the  $x = 0.8$  and  $1$  samples were those of the rhombohedral  $\text{BiFeO}_3$  type. Both monoclinic and rhombohedral phases coexisted in the  $x = 0.75$  sample, consistent with the results of MOCVD thin films.<sup>16)</sup> Interestingly, the separation of the 001 and 100 peaks in the tetragonal phases  $x = 0$  to  $0.6$  did not change apparently with increasing  $x$ . The lattice constants of the tetragonal phases were refined and are plotted in Fig. 2(a) with  $c/a$  ratio. This shows that  $c/a$  ratio slightly decreases with increasing  $x$ . On the other hand, the spontaneous polarization calculated from the refined atomic positions assuming a point charge model increased from  $130\text{ }\mu\text{C}/\text{cm}^2$  for  $x = 0$  to  $133\text{ }\mu\text{C}/\text{cm}^2$  for  $x = 0.5$ .

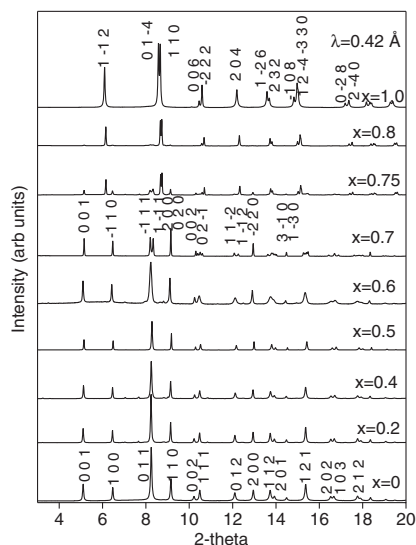


Fig. 1. SXRD patterns of  $\text{BiCo}_{1-x}\text{Fe}_x\text{O}_3$  ( $x = 0, 0.2, 0.4, 0.5, 0.6, 0.7, 0.75, 0.8$ , and  $1.0$ ) taken at room temperature. The indexes for the tetragonal  $\text{BiCoO}_3$  type phase, monoclinic  $\sqrt{2}a \times \sqrt{2}a \times a$  phase and rhombohedral  $\text{BiFeO}_3$  type phase are shown on the top of the peaks.

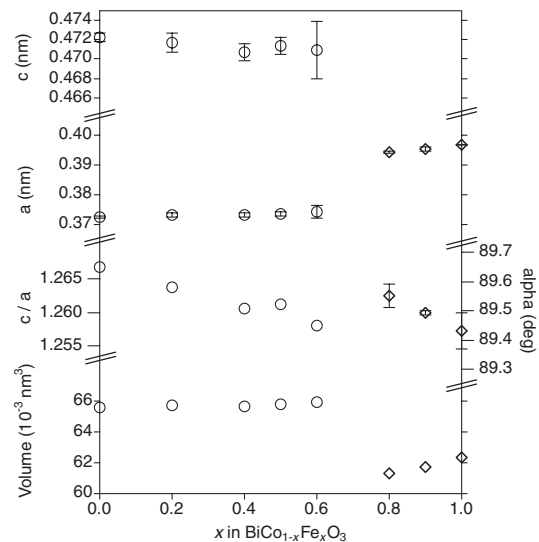


Fig. 2. Composition dependences of lattice parameters,  $c/a$  ratio, and unit cell volume of  $\text{BiCo}_{1-x}\text{Fe}_x\text{O}_3$ .

Figure 3 shows the XRD patterns for the  $x = 0.7, 0.8$ , and  $0.9$  samples at elevated temperatures. For the  $x = 0.7$  sample, the splitting of the tetragonal 011 peak disappeared at  $200^\circ\text{C}$  indicating the conversion from the monoclinic to the tetragonal structure. The tetragonal phase was stable up to  $600^\circ\text{C}$  but several new peaks, with the two most intense peaks being marked by circles, appeared at  $700^\circ\text{C}$ . The  $x = 0.8$  sample gradually changed from the rhombohedral  $\text{BiFeO}_3$ -type phase to the tetragonal one in the temperature range of  $250$  to  $700^\circ\text{C}$ . The peaks for the unidentified phase as found in the  $x = 0.7$  sample appeared at  $700^\circ\text{C}$  and finally the system changed to cubic at  $850^\circ\text{C}$ . Since  $\text{BiCoO}_3$  is known to decompose to  $\text{Co}_3\text{O}_4$  and  $\text{Bi}_{25}\text{CoO}_{39}$  at  $450^\circ\text{C}$  with no structural change, this is the first observation of ferroelectric transition in  $\text{BiCoO}_3$ -containing tetragonal phase. There is an unidentified intermediate phase between the tetragonal and cubic phases. The  $x = 0.9$  sample was rhombohedral below the cubic transition temperature of  $750^\circ\text{C}$ . It decomposed to  $\text{Bi}$ ,  $\text{Fe}_2\text{O}_3$ ,  $\text{Fe}_3\text{O}_4$ , and unidentified phases above  $950^\circ\text{C}$ .

On the basis of results of the high-temperature XRD analysis, we made a tentative phase diagram, as shown in Fig. 4. The tetragonal  $x = 0$  to  $0.7$  samples decomposed without changing to the cubic phase, while a tetragonal-to-cubic phase transition was observed for the  $x = 0.8$  sample. The tetragonal–rhombohedral phase boundary lies between  $x = 0.6$  and  $0.8$  at room temperature while it is between  $x = 0.8$  and  $0.9$  at  $700^\circ\text{C}$ . It is suggested that this phase boundary is the MPB line. Although dielectric and piezoelectric measurements are indispensable for establishing this binary system as a MPB system, this finding will open a new direction in the search for new lead-free piezoelectric materials. The phase boundary is almost vertical in the composition–temperature phase diagram suggesting the temperature stability of the piezoelectric property, as observed in PZT. Further tuning of the phase boundary and  $T_C$  by chemical modification is left for the future study.

### 4. Conclusions

The composition–temperature phase diagram of the

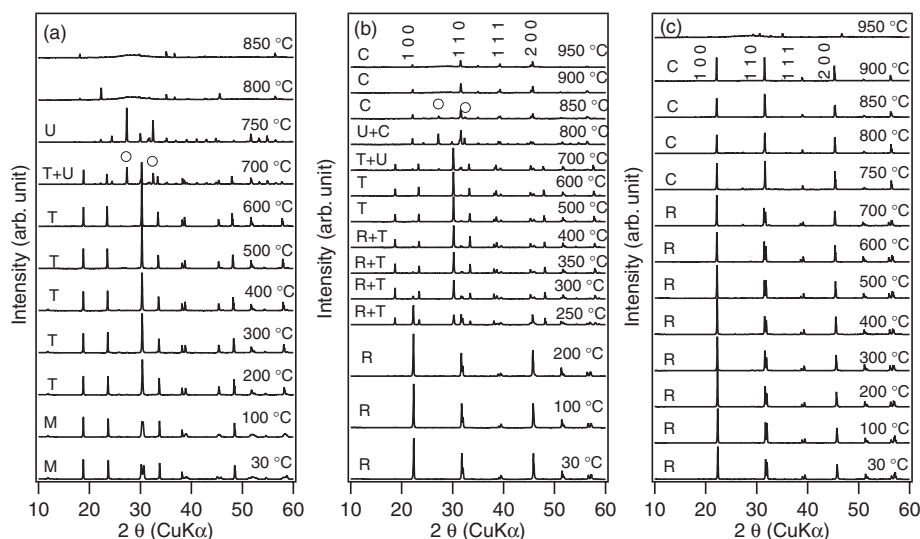


Fig. 3. Temperature dependences of the laboratory XRD patterns of (a)  $\text{BiCo}_{0.3}\text{Fe}_{0.7}\text{O}_3$ , (b)  $\text{BiCo}_{0.2}\text{Fe}_{0.8}\text{O}_3$ , and (c)  $\text{BiCo}_{0.1}\text{Fe}_{0.9}\text{O}_3$ . M, T, U, R, and C stand for the monoclinic, tetragonal, undefined, rhombohedral, and cubic phases, respectively.

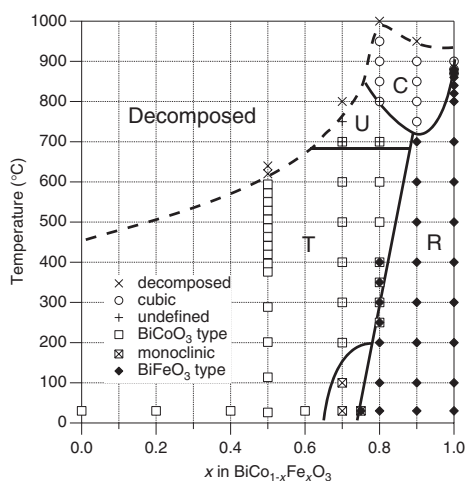


Fig. 4. Composition-temperature phase diagram for  $\text{BiCo}_{1-x}\text{Fe}_x\text{O}_3$  system. C, T, and R stand for the cubic, tetragonal, and rhombohedral phases, respectively.

$(1-x)\text{BiCoO}_3-x\text{BiFeO}_3$  system was investigated. Samples with  $x = 0$  to  $0.6$  had tetragonal  $\text{BiCoO}_3$  structures, while those with  $x = 0.8$  to  $1$  had rhombohedral  $\text{BiFeO}_3$  structure at room temperature. The  $x = 0.7$  sample had a monoclinic  $\sqrt{2}a \times \sqrt{2}a \times a$  cell, the same as the low temperature phase of the MPB composition of PZT. The tetragonal-to-cubic phase transition was first observed in Bi-based perovskite for the  $x = 0.8$  sample. It was found that the tetragonal-rhombohedral phase boundary lies between  $x = 0.7$  and  $0.9$ . The tetragonal-cubic transition temperatures at the phase boundary of  $700$ – $850^\circ\text{C}$  are the highest among those of known binary perovskite systems.

### Acknowledgements

We thank Professor Nobuhiro Kumada and Rigaku Co. for the assistance with the high-temperature XRD study. This work was partially supported by Grants-in-Aid from the Ministry of Education, Culture, Sports, Science and Technology, Japan for Scientific Research (Nos. 17105002,

18350097, 19GS0207, 19014010, 19340098, and 19052008) and for a Joint Project of the Chemical Synthesis Core Research Institutions and the Elements Science and Technology Project. The synchrotron radiation experiments were performed at SPring-8 with the approval of the Japan Synchrotron Radiation Research Institute.

- 1) B. Jaffe, W. R. Cook, and H. Jaffe: *Piezoelectric Ceramics* (Academic, London, 1971).
- 2) R. E. Eitel, C. A. Randall, T. R. Shrout, P. W. Rehrig, W. Hackenberger, and S. Park: *Jpn. J. Appl. Phys.* **40** (2001) 5999.
- 3) R. E. Cohen: *Nature* **358** (1992) 136.
- 4) P. Goudochnikov and A. J. Bell: *J. Phys.: Condens. Matter* **19** (2007) 176201.
- 5) Y. Saito, H. Takao, T. Tani, T. Nonoyama, K. Takatori, T. Homma, T. Nagaya, and M. Nakamura: *Nature* **432** (2004) 84.
- 6) J. Wang, J. B. Neaton, H. Zheng, V. Nagarajan, S. B. Ogale, B. Liu, D. Viehland, V. Vaithyanathan, D. G. Schlom, U. V. Waghmare, N. A. Spaldin, K. M. Rabe, M. Wuttig, and R. Ramesh: *Science* **299** (2003) 1719.
- 7) V. V. S. Sai Sunder, A. Halliyal, and A. M. Umarji: *J. Mater. Res.* **10** (1995) 1301.
- 8) X. Long and Z. G. Ye: *Chem. Mater.* **19** (2007) 1285.
- 9) T. R. Shrout and S. J. Zhang: *J. Electroceram.* **19** (2007) 113.
- 10) M. Azuma, K. Takata, T. Saito, S. Ishiwata, Y. Shimakawa, and M. Takano: *J. Am. Chem. Soc.* **127** (2005) 8889.
- 11) M. Sakai, A. Masuno, D. Kan, M. Hashisaka, K. Takata, M. Azuma, M. Takano, and Y. Shimakawa: *Appl. Phys. Lett.* **90** (2007) 072903.
- 12) S. Ishiwata, M. Azuma, M. Takano, E. Nishibori, M. Takata, M. Sakata, and K. Kato: *J. Mater. Chem.* **12** (2002) 3733.
- 13) M. Azuma, S. Carlsson, J. Rodgers, M. G. Tucker, M. Tsujimoto, S. Ishiwata, S. Isoda, Y. Shimakawa, M. Takano, and J. P. Attfield: *J. Am. Chem. Soc.* **129** (2007) 14433.
- 14) A. A. Belik, M. Azuma, T. Saito, Y. Shimakawa, and M. Takano: *Chem. Mater.* **17** (2005) 269.
- 15) A. A. Belik, S. Iikubo, K. Kodama, N. Igawa, S. Shamoto, S. Niitaka, M. Azuma, Y. Shimakawa, M. Takano, F. Izumi, and E. Takayama-Muromachi: *Chem. Mater.* **18** (2006) 798.
- 16) S. Yasui, K. Nishida, H. Naganuma, S. Okmura, T. Iijima, and H. Funakubo: *Jpn. J. Appl. Phys.* **46** (2007) 6948.
- 17) E. Nishibori, M. Takata, K. Kato, M. Sakata, Y. Kubota, S. Aoyagi, Y. Kuroiwa, M. Yamakata, and N. Ikeda: *Nucl. Instrum. Methods Phys. Res., Sect. A* **467–468** (2001) 1045.
- 18) F. Izumi and T. Ikeda: *Mater. Sci. Forum* **321–324** (2000) 198.
- 19) B. Noheda, J. A. Gonzalo, L. E. Cross, R. Guo, S.-E. Park, D. E. Cox, and G. Shirane: *Phys. Rev. B* **61** (2000) 8687.